Crooked-line 2D seismic reflection imaging in crystalline terrains: Part 2, migration

Mladen R. Nedimović* and Gordon F. West‡

ABSTRACT

Seismic reflection surveys are frequently conducted over very complicated geological structure, but surveying often must be confined to existing crooked roads or tracks. Typically, data from such 2D crooked-line surveys are processed using standard common midpoint (CMP) stacking techniques to obtain a 2D time section which is then 2D migrated. In Part I, we show that a reflector dip component across the processing line can cause serious problems for standard CMP stacking. We also propose a supplementary processing step in which cross-dip is determined locally and cross-dip moveout (CDMO) is removed from data to form an optimum cross-dip stack. However, a crooked-line survey is really a swath 3D survey, and ideally we would like to obtain a 3D image of reflectivity surrounding the profile.

Here we investigate the potential of 3D prestack Kirchhoff migration to directly image all observed reflections; i.e., we attempt to construct a 3D image volume of all reflectors viewed by the survey. Because reflectors that face away from the acquisition line cannot return much wave energy from available sources to available receivers, they cannot be imaged even if they lie directly beneath the survey profile. Tests show that the cross-profile spread of trace midpoints usually is sufficient to provide a useful degree of cross-line positioning of reflection points. A very helpful image volume is thus obtained.

Kirchhoff 3D prestack migration is computationally laborious. A much quicker but less complete method is to create the 3D migrated image volume from the 2D optimum cross-dip stack and the associated set of cross-dips. Robustness of migration methods to time errors in the prestack data traces such as poorly corrected statics is also an issue. Tests show that in difficult cases, particularly where only 2D processing is warranted, migration of trace absolute amplitude rather than standard phase data may lead to a superior result.

INTRODUCTION

In the companion paper (Nedimović and West, 2003; hereafter, Part I), we discuss the problems of imaging reflectors in crystalline igneous metamorphic terrain from 2D seismic data acquired on crooked lines. We show that the cross-profile dip of reflectors can severely damage CMP stacking of the data. We also describe a process for determining reflector cross-dip by a semblance-based method and then correcting for the crossdip moveout (CDMO) in the stack. In this way we obtain what we called a locally optimum cross-dip stacked section on which to base interpretation.

However, a high-fold 2D seismic reflection survey on a crooked line is really a limited swath 3D investigation of the subsurface reflectivity near the acquisition line. Optimistically, because structures in crystalline terrain can be very complex, one would like to obtain some sort of 3D image of structure by 3D migrating the seismic data. Of course, this could be impractical because of the inherent limitations of the observational data set. Swath 3D data have a very small cross-profile aperture, an uneven distribution of source–receiver midpoints, and a small range of source–receiver azimuths, so migration might be fruitless.

Standard prestack 3D migration is a very cumbersome and expensive computational process. Therefore, in addition to testing standard 3D prestack migration, we have also studied the feasibility of migrating the locally optimum crossdip stack of Part I into a 3D volume. Furthermore, we have

tested migration of amplitude stacks, sections formed by averaging trace absolute amplitude in CMP gathers. A summary flowchart of the different approaches to processing crooked line data is shown in Figure 1. Our experiments indicate that all three migration processes can be useful.

Nevertheless, our tests on both synthetic and field data suggest that the most effective approach to imaging 2D crooked-line survey data is first to produce an optimum cross-dip stack. Then, if cross-dip information can be extracted for many reflectors, and especially if overlapping events are abundant, investing the CPU power to prestack-migrate the data into a 3D volume will very likely be worthwhile.

The data

Our field survey example is the high-resolution Sturgeon Lake line. It is a short but densely recorded profile acquired for mineral exploration research. A fixed spread of 393 receiver traces spaced at 20-m intervals recorded explosive shots spaced every 40 m. Average CMP bin fold reached well over 100 traces per gather. The acquisition profile is locally very crooked, but it oscillates about a straight processing line. Figure 1a in Part I shows both the acquisition and the processing lines on a map of the surface geology.

All synthetic survey data used in our tests were computed using a ray-Born method. The survey geometry of either the Sturgeon Lake line or Abitibi line 23 was assumed (see Part I). The reflectors modeled range from a few point diffractors to groups of several rectangular planes. In all cases, the host medium was assumed to have constant velocity. For more details about the modeling and the field surveys, see the introduction and appendices A and B of Part I.

Migration of swath 3D data

The idea that a 3D structural image might be obtained from a 2D crooked-line seismic data set is not novel. For instance, Geiger et al. (1995) and Bancroft et al. (1998) suggest the possibility. However, we are unaware of published examples, and the concept appears to have remained more hypothetical than practical. Certainly, there are fundamental limitations to what can be achieved from a 2D crooked-line data set, and there are reasons to worry about the quality of any 3D image obtained from such data. We discuss these limitations and concerns below. Basically, they reduce to

1) lack of observations from viewpoints that can generate Snell's law reflections from whatever dipping interfaces are in the ground;
2) lack of sufficient cross-line horizontal aperture in the data set to resolve the cross-line position of reflectors; and
3) irregular spatial distribution of the data.

The first and second points are fundamental to any swath 3D survey. The third condition results when shot and receiver positions are confined to a single (albeit crooked) survey line.

The Kirchhoff migration method seems, at least from an operational view, to be usable with irregularly distributed data. This summation process relies on interference to remove unwanted parts of the signal from the final image product. According to the traveltime of each datum value in a data trace, reflectivity amplitude is inserted into the image space at every space point that could possibly have generated that particular datum. Then, when the putative reflectivity contributions from all data have been included in the image, interference will enhance the total reflectivity signal at locations where the reflections actually occurred and attenuate it elsewhere. For this to happen, the survey data traces must be distributed evenly enough throughout a large enough spatial range (aperture). The required aperture is a function of wavelength and distance to the reflector. If the acquisition geometry does not provide the minimum required aperture, extended smears of reflectivity values will be left in the migrated image that indicate only where the reflection points might be located, not where they actually are.

If a straight-line 2D survey is conducted in geological terrain for which no assumptions can be made about cross-line structure, the position of any observed reflectors will be completely ambiguous in a cylinder surrounding the acquisition/processing line. Also, no assurance can be given that all reflectors that cut the vertical section containing the survey profile will be imaged by the survey, because only those that directly face some part of the survey line will generate appreciable signal.

In applying 3D migration to 2D crooked-line data, we are hoping the survey geometry will provide enough cross-line aperture so reflection points can be reasonably well positioned in the cross-line direction. However, the degree of localization achieved in the cross-line direction will likely be much less than along the survey profile. Furthermore, it should be expected to vary along the profile with the specific crookedness of the acquisition line.

The 3D migration of the original prestack data volume with a 3D laterally varying velocity model is a very computationally expensive way to obtain a 3D image volume from the data. The usual reasons for making such an effort are significant lateral velocity variations and very steep reflector dips. However, velocity is not an important factor in our case. In crystalline terrains, the average velocity over a path of several hundred meters in the depth range from 0.5 to 10 km usually varies less than a few percent, so constant velocity or rms velocity migration is often sufficient. With this simplification,

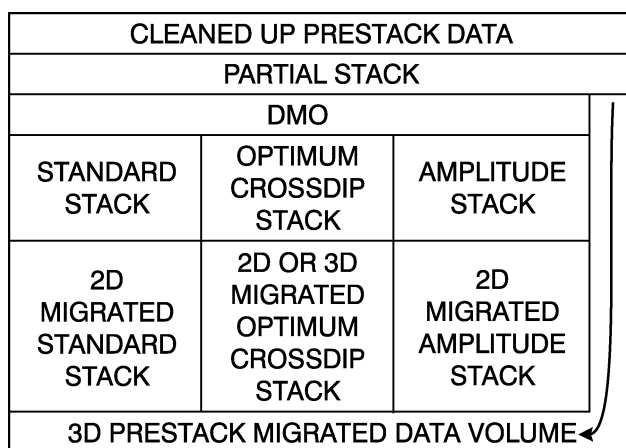| CLEANED UP PRESTACK DATA		
PARTIAL STACK		
DMO		
STANDARD STACK	OPTIMUM CROSSDIP STACK	AMPLITUDE STACK
2D MIGRATED STANDARD STACK	2D OR 3D MIGRATED OPTIMUM CROSSDIP STACK	2D MIGRATED AMPLITUDE STACK
3D PRESTACK MIGRATED DATA VOLUME		

FIG. 1. Processing flowchart summarizing both the standard and the suggested alternative approaches to processing 2D crooked-line data.

3D migration becomes feasible using only workstation-level computers.

As a more economical alternative to 3D prestack migration, we have explored poststack migration of the 2D optimum cross-dip stack into a 3D volume. This is accomplished by using the cross-slowness information provided in the composite cross-dip image together with the actual cross-line spread extent. In effect, a 3D presentation of the 2D data section is produced together with some indication of the inherent positional ambiguity.

Although useful results can be obtained with the poststack procedure, it has fundamental limitations. For instance, where the reflection responses of the imaged events overlap in the section, only the stronger will remain in the optimum cross-dip stack and the 3D image; also, to independently determine NMO, DMO, and CDMO, an azimuthal approximation must be made. Signal loss from these limitations/approximations cannot be recovered by any poststack 3D migrator.

In Part I, we showed that converting partially stacked CMP trace data into absolute amplitudes and then stacking to obtain an amplitude section is effective in some cases where time errors in the data are too abundant or too unpredictable to be corrected before stack. In this paper, we show that poststack migration can be successfully applied to amplitude stacks. Similarly, absolute amplitude trace data of partially stacked CMP gathers can be migrated by a prestack process. As with amplitude stacking, amplitude migration can sometimes be useful as a process of last resort.

METHODOLOGY

3D prestack migration.—We have carried out our 3D prestack migrations by applying a standard 3D rms velocity Kirchhoff migration method to the observational data. As shown in Figure 2, the input 2D crooked-line survey has data traces distributed unevenly in a swath around the acquisition line; the output 3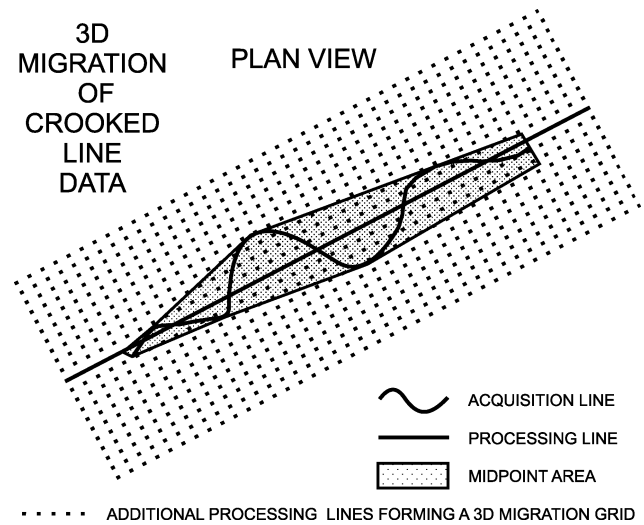D prestack migrated volume is an evenly distributed grid of image data traces aligned with the 2D processing (slalom) line.

To minimize the computational load of the prestack migration, and also to smooth out some of the great bin density variations of trace midpoints inherent to crooked line geometry, we first perform an NMO-corrected partial stack on the cleaned-up prestack observational data. In any CMP bin gather along the processing line, there is a strong correlation of midpoint cross-line offset with source–receiver offset; so partial stacking into narrow ranges of source–receiver offset only averages traces with quite similar cross-line offsets. Thus, all reflection signals should remain well preserved for migration.

When designing the output migration image grid, it is very helpful to have already obtained the optimum cross-dip stack for the survey. It helps decide how extensive the output grid needs to be so run time can be minimized.

Unlike the schematic shown in Figure 2 and our Sturgeon Lake field data, most crooked-line surveys are sufficiently long
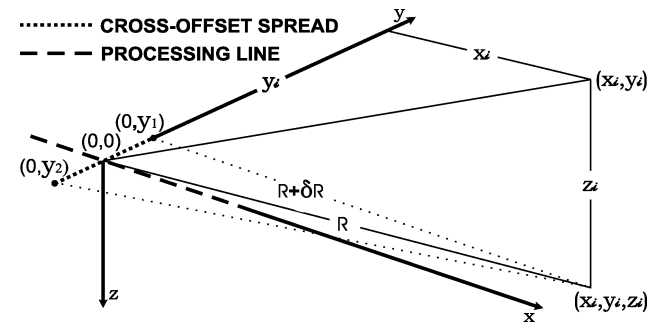

FIG. 3. Geometry for 3D poststack migration. The origin of space coordinates $(0, 0)$ is the location on the processing line of the selected trace in the 2D stacked section. The image point (x_i, y_i, z_i) is at distance R from it. Points $Y_1(0, y_1)$ and $Y_2(0, y_2)$ mark the cross-line range of individual trace midpoints in the CMP bin gather of the stacked trace.
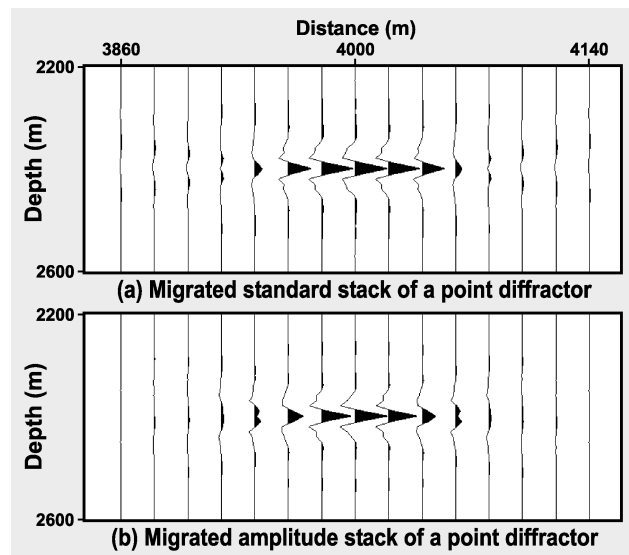

FIG. 4. Images obtained by migrating the signal from a point diffractor. (a) Migrated standard stack. (b) Migrated amplitude stack. The results are similar.

FIG. 2. Midpoint geometry of a crooked-line survey with the output data array for 3D migration (schematic).

to require a multisegment processing line. This can complicate the 3D prestack migration process since separate 3D output volumes and separate migration processes for each grid may be needed.

3D poststack migration.—A more economical but potentially less effective method of obtaining a 3D reflectivity volume from 2D crooked-line data is to apply a 3D poststack migration to the traces of the locally optimum cross-dip
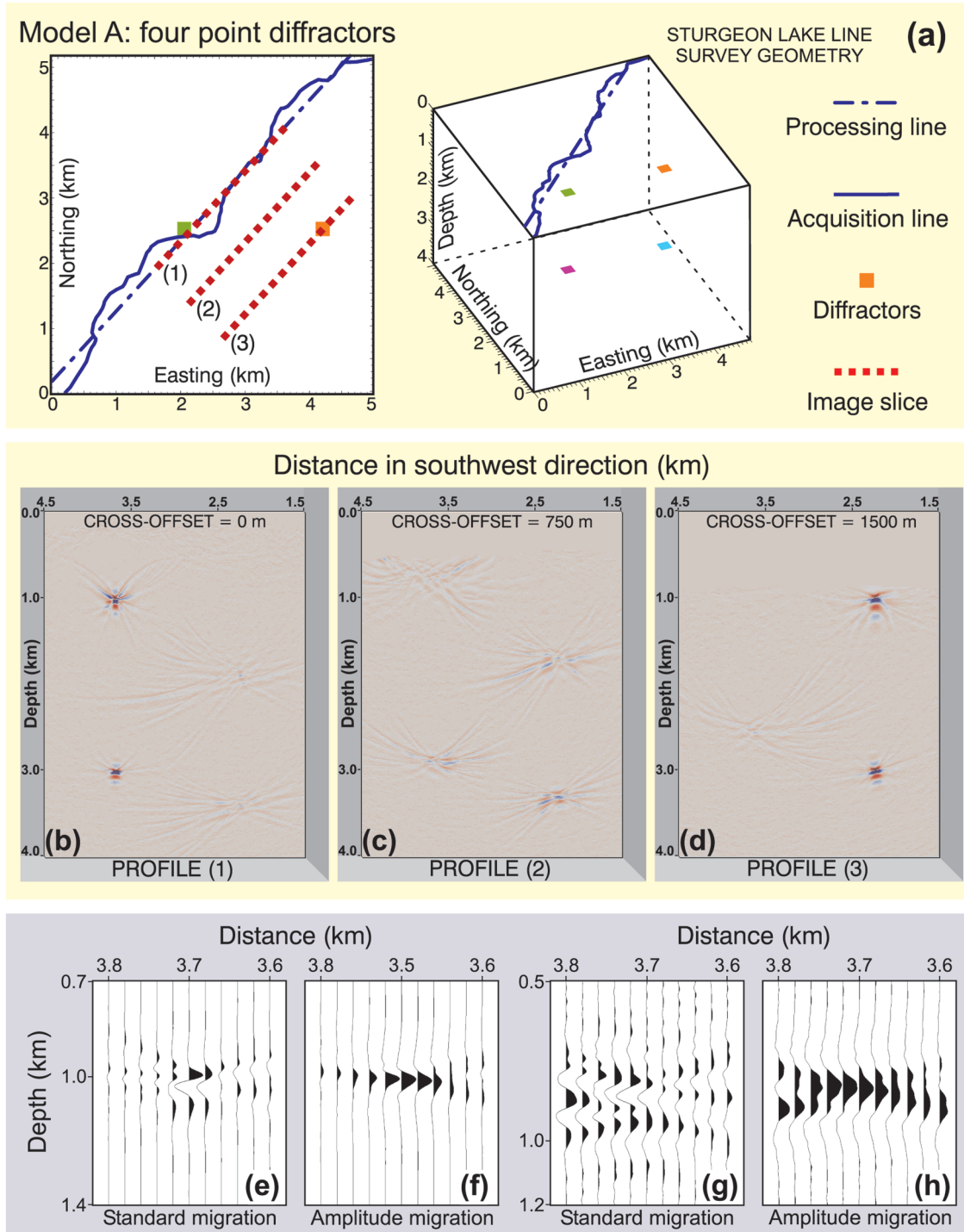

FIG. 5. Imaging of four point scatterers by 3D prestack migration. (a) Plan and perspective view of model A and the image slices. (b, c, d) In-line slices (1), (2), and (3) in variable density format. The color palette is given in Figure 9. (e, f, g, h) Close-ups of the upper event under the processing line. Parts (e) and (f) are the result of standard and amplitude migration, respectively; parts (g) and (h) are the same except that time shifts simulating static errors have been included.

stack. Contributions to the migrated image from each of the 2D stacked traces are computed as if a stacked trace were the average of a group of individual traces uniformly spaced over the cross-line width of the CMP bin and as if the events on those traces shift in time with cross-line offset according to the cross-slowness found for each event by the optimum cross-dip analysis. Modifying the standard Kirchhoff poststack migration to do this is straightforward and is described below. The output 3D grid for poststack migration is chosen in the same way as for 3D prestack migration. It may be necessary to apply a bandpass and coherency filter to the input optimum cross-dip stack to prevent spatial aliasing on the output grid.

Figure 3 shows the geometry for one image point in the 3D image space and one trace from the optimum cross-dip stacked data. The datum value to be migrated to the image point at (x_i, y_i, z_i) is found on the data trace at $(0,0)$ at time $t = 2R/v_{\mathrm{rms}}$, where v_{rms} is the root mean square velocity and R is the distance from the stacked trace to the image point. The event on the (imaginary) traces distributed over the cross-line $Y_1(0, y_1)$–$Y_2(0, y_2)$ and contributing to the stacked trace would have been found at time t shifted by δt, the product of the cross-line offset y_c and the optimum cross-slowness p_t estimated for each t in the trace at $(0,0)$ by the optimum cross-dip analysis. The contributions to the image point by all (imaginary) traces in the gather are summed. The change of R to $R + \delta R$ for each trace can be approximated by using the binomial series:

$$
\begin{aligned}
R + \delta R &= \left(x_i^2 + (y_i - y_c)^2 + z_i^2 \right)^{\frac{1}{2}} \\
&= R \left(1 - \frac{2 y_i y_c}{R^2} + \frac{y_c^2}{R^2} \right)^{\frac{1}{2}} \quad (1) \\
&\simeq R \left(1 - \frac{2 y_i y_c}{R^2} + \frac{y_c^2}{2 R^2} \right).
\end{aligned}
$$

Thus, the total time shift equals

$$
\delta t = 2 p_t y_c - \frac{2 y_i y_c}{v_{\mathrm{rms}} R} + \frac{y_c^2}{v_{\mathrm{rms}} R}. \quad (2)
$$

By substituting y_1 and y_2 instead of y_c, the extreme time shifts are found. Data in the time window $(t + \delta t)_{\max}$ to $(t + \delta t)_{\min}$ are averaged and added to the image point (x_i, y_i, z_i). The averaging acts as a focusing filter for migration. The process is repeated for each output image point and for all data samples of every trace of the optimum cross-dip stack.

Amplitude migration.—Migration of trace absolute amplitude has rarely been contemplated, perhaps because absolute trace amplitudes do not behave linearly in sums of signals. Thus, combining absolute amplitudes does not have a basis in wave theory. However, geometrical migration of the density or opaqueness of event lines or curves has a perfectly good foundation in Radon transform theory.
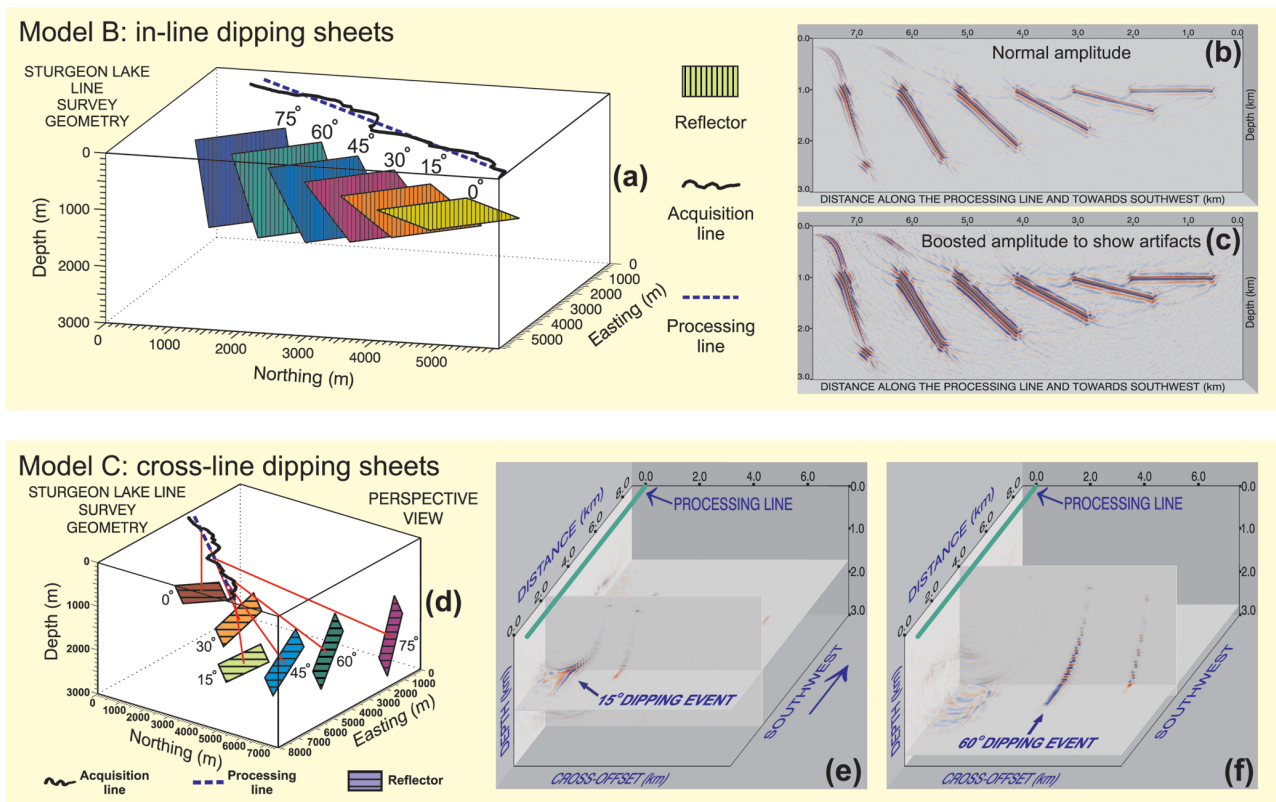

FIG. 6. Imaging of dipping reflectors by 3D prestack migration. (a) Six reflecting plates dipping along the processing line. (b, c) Slice of the processing line from the 3D prestack migrated image volume at medium and high plot sensitivity. (d) Six cross-line dipping reflectors that face toward the acquisition/processing line and lie approximately northwest of it. (e, f) Some in-line and cross-line slices of the image volume.

This suggests that the 2D amplitude stacks discussed in part I, as well as the absolute amplitudes of partially stacked CMP trace data, might be successfully migrated in the same fashion as standard data. However, amplitude envelope traces will need to be frequency filtered before migration. The filtering must remove the zero frequency component or dc shift of the amplitude trace while retaining low frequencies that correspond to time variations of the trace envelope. Traces may also be smoothed to eliminate rectification noise. This can be achieved with a trapezoid bandpass filter in which the low cut is set at 0 Hz and the low-frequency corner is set lower than for standard phase data. High cut and high pass frequencies can be determined experimentally for each data set.

Before migration, the trace amplitudes should be normalized by automatic gain control (AGC). If spuriously large amplitude events in the stacked data remain after AGC, raising the values to some arbitrary positive power less than unity tends to improve the migrated amplitude stack.

Figure 4 provides a simple demonstration of migration applied to amplitude traces. It shows 2D poststack migrated standard and amplitude stacks of a single point diffractor. Both results exhibit approximately the same focusing.

The diffractor was positioned directly below the middle of the line at a depth of 2400 m and a 10- to 150-Hz Klauder wavelet was applied. Unlike all the other synthetic data shown in this paper, this set was produced by using a straight-line survey geometry and a regular surface sampling with no shot

or receiver skips. The data were stacked in the normal way. Absolute amplitudes were raised to a power of 1.5 before amplitude stacking. After stacking, both the standard and the amplitude section were 2D migrated using a standard phase shift algorithm. To achieve the good focusing shown in the figure, bandpass filtering was applied twice to the amplitude data: first to the input amplitude stack (0-20-120-150 Hz) and then to the migrated section (5-15-40-50 cycle/km). The same postmigration bandpass filter was applied to the migrated standard stack.

MIGRATION OF SYNTHETIC DATA

Point diffractors.—In our first test of 3D prestack migration, the modeled data consist of the seismic response of four point diffractors. The crooked-line geometry of the Sturgeon Lake line was assumed. Two of the diffracting points are approximately under the processing line, and two are offset ~1500 m to one side. The shallower diffractors are buried 1000 m; the deeper ones, 3000 m. The model and results are shown in Figure 5. The main goal was to learn if standard and/or amplitude 3D Kirchhoff migration could clearly differentiate between a diffractor that lies below the acquisition/processing line and one that is laterally offset from it. Only three planes of the migrated data volume were computed.

Figures 5b–d show three vertical slices of the migrated image parallel to the processing line and 750 m apart. The first
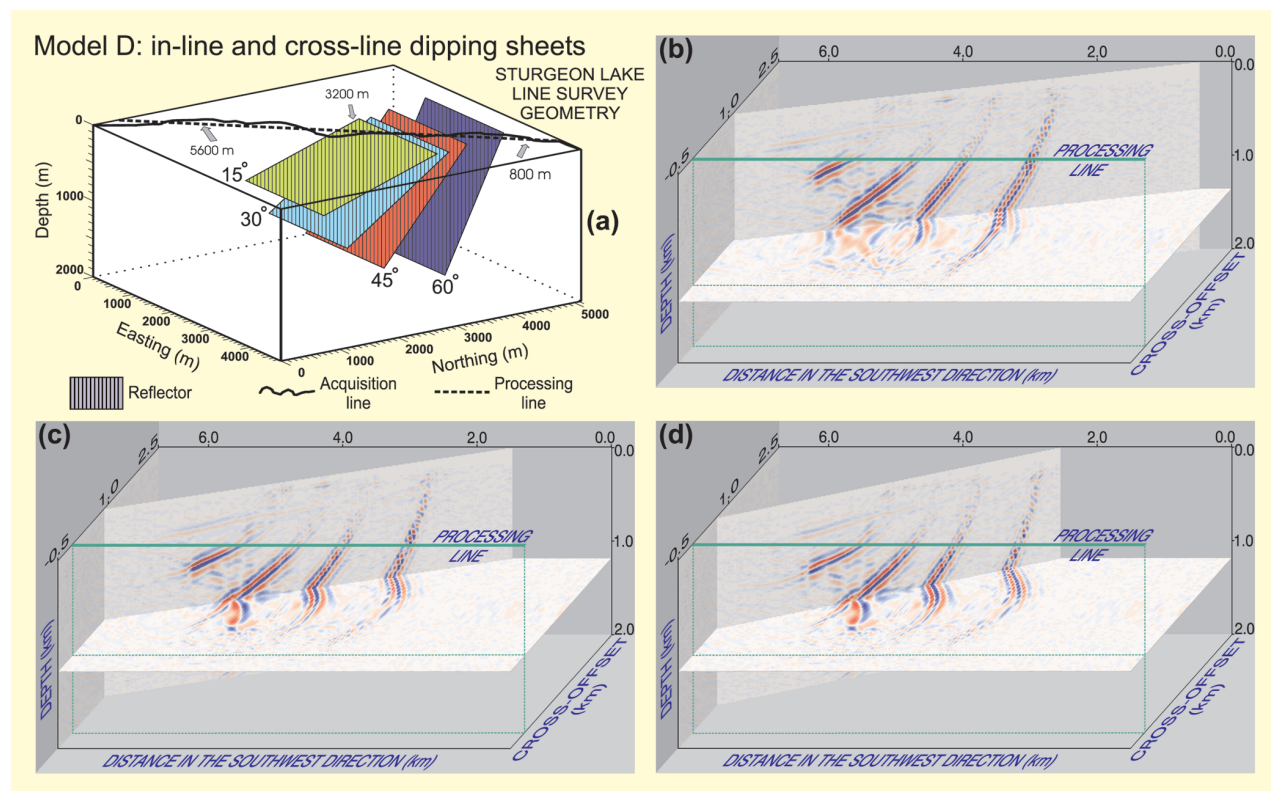

FIG. 7. Imaging reflectors with both in-line and cross-line dip. (a) Four plate-like reflectors that dip south at 15°, 30°, 45°, and 60° across the southwest directed processing line. (b, c, d) Three perspective views of slices of the 3D prestack migrated image volume. The vertical slice has been rotated to show the different parts of the reflector images. All reflectors are easily distinguished and well delineated.

and third image slices contain the actual diffraction points. Slice 2 is positioned midway between to check on the expected cross-line smearing of the images. To make artifacts visible, plot amplitude was significantly increased, so dark parts are oversaturated. Slices 1 (Figure 5b) and 2 (Figure 5c) show images in accord with what 2D in-line migration theory predicts. The events in slice 1 are well focused at their true subsurface positions. As expected, there are artifacts in slice 2 between the diffractors. However, they are much weaker than the main events. The focusing in slice 3 (Figure 5d) at the true position of the diffractors is surprisingly good, considering the irregularity of the survey geometry and the small average swath width of the survey (∼350 m).

To see if the result is robust to time errors and to compare standard and amplitude migration, a second test was conducted. In it, the static corrections estimated for the Sturgeon Lake line field data were added to the synthetic data before the partial stack, as if they were uncorrectable. Figures 5e–h, show magnified images of the shallow diffraction point closest to the processing line after standard and amplitude migration on data with and without time errors. With no time error, the image of the scatterer focuses well in both standard (Figure 5e) and amplitude data (Figure 5f). With the simulated static error, focusing is seriously damaged regardless of the type of migrated data [standard (Figure 5g) or amplitude (Figure 5h)]. Nevertheless, the amplitude migration focuses better, which again suggests that a migration of amplitude data may be more robust to error.

In-line dipping reflectors.—The next model contains six in-line dipping platelike reflectors in the geometry of the Sturgeon Lake line (Figure 6a). All reflectors are squares with 1500-m sides and a top edge at 1000 m. They dip in the in-line direction at 0°, 15°, 30°, 45°, 60°, and 75°.

Figures 6b and 6c show slices of the migrated data along the processing line at medium and high sensitivity. In spite of the shortness of the acquisition line (∼8 km), standard 3D prestack migration accurately captures most of the in-line dipping events below the slalom line. A somewhat longer survey would be necessary to completely image the two steepest events. Even at high plot sensitivity, artifacts are not strongly visible. However, we have not shown image slices on either side of the reflectors. The 3D image of the reflectors may be laterally smeared from insufficient cross-line aperture or be attenuated before reaching the true edges of the reflectors because of problems in facing direction.

Cross-line dipping reflectors.—The model consists of six cross-dipping reflectors and the geometry of the Sturgeon Lake line (Figure 6d). The reflectors are the same size and depth as in the in-line case and were placed to northwest of the survey line so they would face the survey profile. The data were prestack migrated to a 3D data volume of 8.8 × 8.0 × 3.0 km. Due to CPU power limitations, the output volume was coarsely sampled (100 m), so some aliasing/undersampling is evident in the result. Vertical and horizontal slices through the migrated 3D volume presented in Figures 6e and 6f are positioned to show images of the 15° and 60° dipping reflectors.

Remarkably, migration was able to position the cross-line dipping reflectors quite accurately in space, but not without

appreciable artifacts and smearing. Although better imaging is usually to be expected for the reflectors with mild or no cross-line dip, all events are imaged comparably. This is because of the positioning of the reflectors in the model relative to the acquisition line. The steeply dipping reflectors face the middle of the survey line, and the horizontal and mildly dipping ones are found at the edges of the survey.

In-line and cross-line dip.—The next model (Figure 7a) was designed to make the imaging process challenging. Four reflectors with similar components of in-line and cross-line dip were
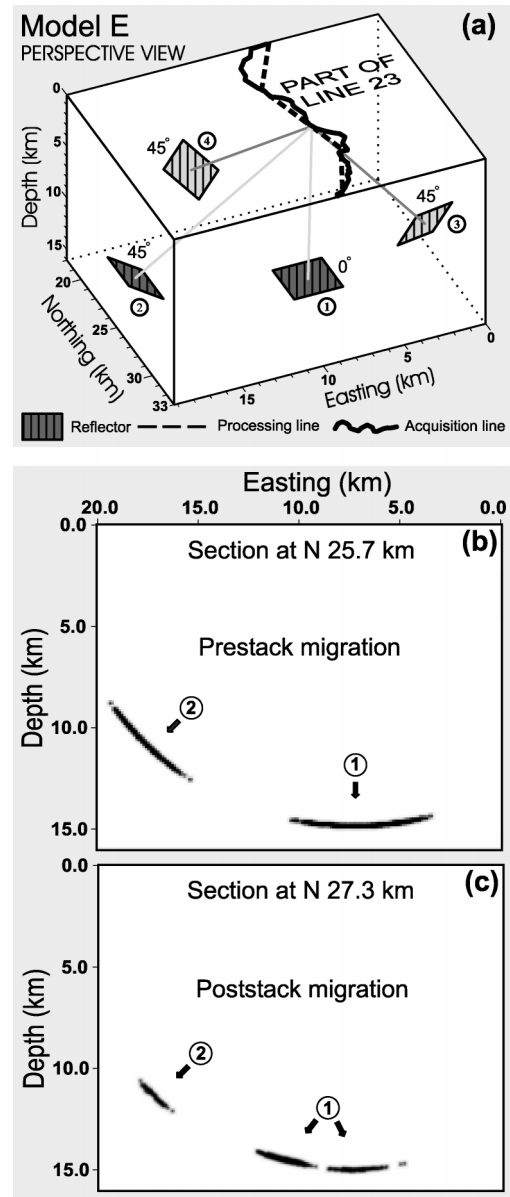

FIG. 8. Comparison of prestack and poststack 3D migration. (a) The model consists of two pairs of reflectors in the Lithoprobe line 23 geometry. (b, c) Cross-line slices through the first pair of reflectors from the 3D prestack migrated and 3D poststack migrated data, respectively. A mild Gaussian blur and toning were applied to these images to make them visible at reduced scale.

placed near the survey profile so at least large parts of them face some part of the survey line. The reflectors are square plates with sides 2000 m long. Their apparent in-line and cross-line dips are ~10.5°, ~20.7°, ~30.0°, and ~37.8°. Because the plates are large and planar, only parts of their surfaces are viewable.

The variety of in-line and cross-line dips in the model ensures that large-magnitude NMO, DMO, and CDMO are present in 2D processing of the data. Because the top parts of the reflectors were placed very close to each other, some of the reflection events overlap in the top of the 2D stacked time section. The optimum cross-dip stack provides a much better image of reflectors than does the standard stack. However,

the image is incomplete wherever there is event interference. Moreover, the approximations made to compute and remove NMO, DMO, and CDMO are not sufficiently accurate when all of these moveouts are very large, so this is a test case where 3D migration would seem to be needed.

The data were prestack depth migrated to a 3D ($6.8 \times 3.0 \times 2.0$ km) data volume. The results are shown Figures 7b–d. All of the reflectors have been well indicated, despite the fact that CPU limitations forced migration of the data to a coarse 3D grid (50-m sample rate) in which aliasing can occur. However, smearing and attenuation because of facing problems certainly are evident.
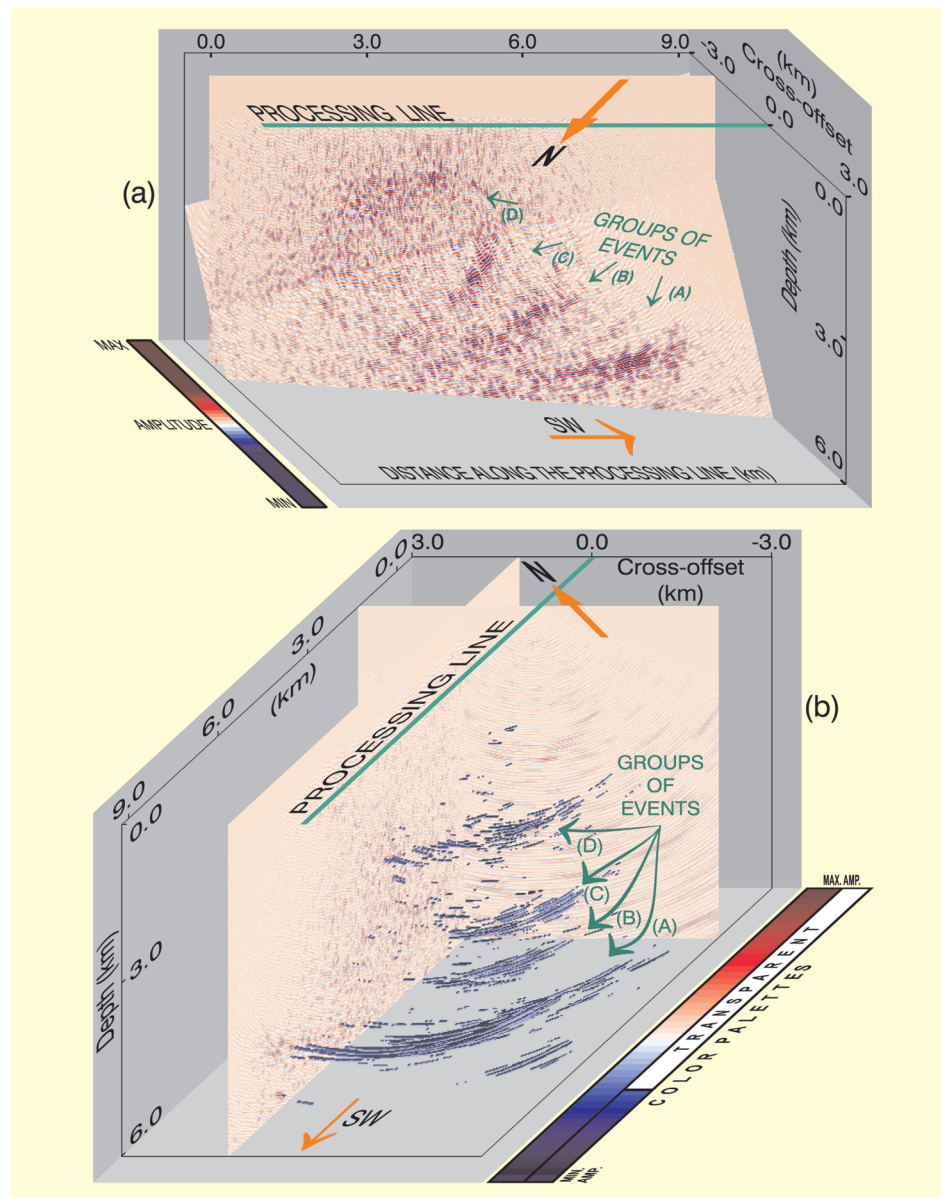

FIG. 9. The 3D prestack migration of Sturgeon Lake line field data. (a, b) Views at the migrated image volume from the north–northeast and southwest–south, respectively. (a) A perspective of variable density slices showing the location of the strongest events. (b) An isosurface presentation of the image data in 3D space with the isosurface threshold set in the midnegative signal range. Opaque variable density slices are inserted to help the reader visualize the position of the main clusters of events. The processing line is superimposed on both images. The appropriate color palette is given for each part of the figure.

Comparison of prestack and poststack 3D migration.—Our final test is a comparison of 3D prestack and 3D poststack migration. The model for it contained two pairs of reflecting plates and used the survey geometry of the northern third of the Lithoprobe Abitibi–Grenville transect, line 23 (Figure 8a). Reflectors 1 and 2 of pair I are relatively far away from the acquisition line. They dip at 0° and 45°, respectively. Reflectors 3 and 4 of pair II are closer to the acquisition line and dip at 45°. For practical purposes, reflector 2 exhibits a pure cross-line dip, while reflectors 3 and 4 dip in both directions equally. All reflectors are square planes with sides 3000 m long. Their reflective responses overlap in the 2D stacked section on the chosen processing line. A 10–56-Hz Klauder wavelet was applied in the modeling.

We have applied both 3D prestack and 3D poststack amplitude migration to the synthetic data to obtain two coarsely sampled (100 m) image volumes (15.0×20.0×16.0 km). Vertical slices of the image volume through reflector pair I are shown in Figures 8b and 8c. As expected, a much better image was provided by the 3D prestack migration. The poststack migration provides a useful image at substantially lower CPU effort, but there is a break in event 1, and event 2 is imaged only partially. The information loss about the overlapping events that occurs in producing the optimum cross-dip stack is permanent and necessarily affects the poststack migrated image. The advantage of the poststack migration is its computational speed. For this reason, it may be used when the resources for a prestack migration are unavailable.

THE FIELD EXAMPLE

The field data of the Sturgeon Lake line, after being sorted into 200-m offset windows and partial stacking, consisted of 342 CMP bin gathers with a maximum fold of 53. The original data were sampled at 1 ms and had useful frequency content of up to ~300 Hz and traces of 3 s length. Our fastest computer at the time we planned to 3D prestack migrate the data was a 330-MHz Sun UltraSparc station 10. To hold the migration run time to something realizable, the size of the output data set was set at $9.7 \times 6.0 \times 6.0$ km, a volume somewhat smaller than originally desired. The spatial sample rate in the image space was set at 18 m in all three directions. Migration rms velocity ranged from 6000 to 6500 m/s. To prevent aliasing in the image volume, a high-cut frequency filter (10-30-80-100 Hz) was applied to the input data.

Two isosurface/slice images of the main events in the 3D prestack migrated data are displayed in Figure 9. Most of the reflection events migrate south from the northeast–southwest processing/acquisition line, and there they display an east–west strike and a northerly dip. The strongest groups of events are labeled A, B, C, and D. All exhibit both in-line and cross-line dip (Figures 9 and 10). The same groups of events
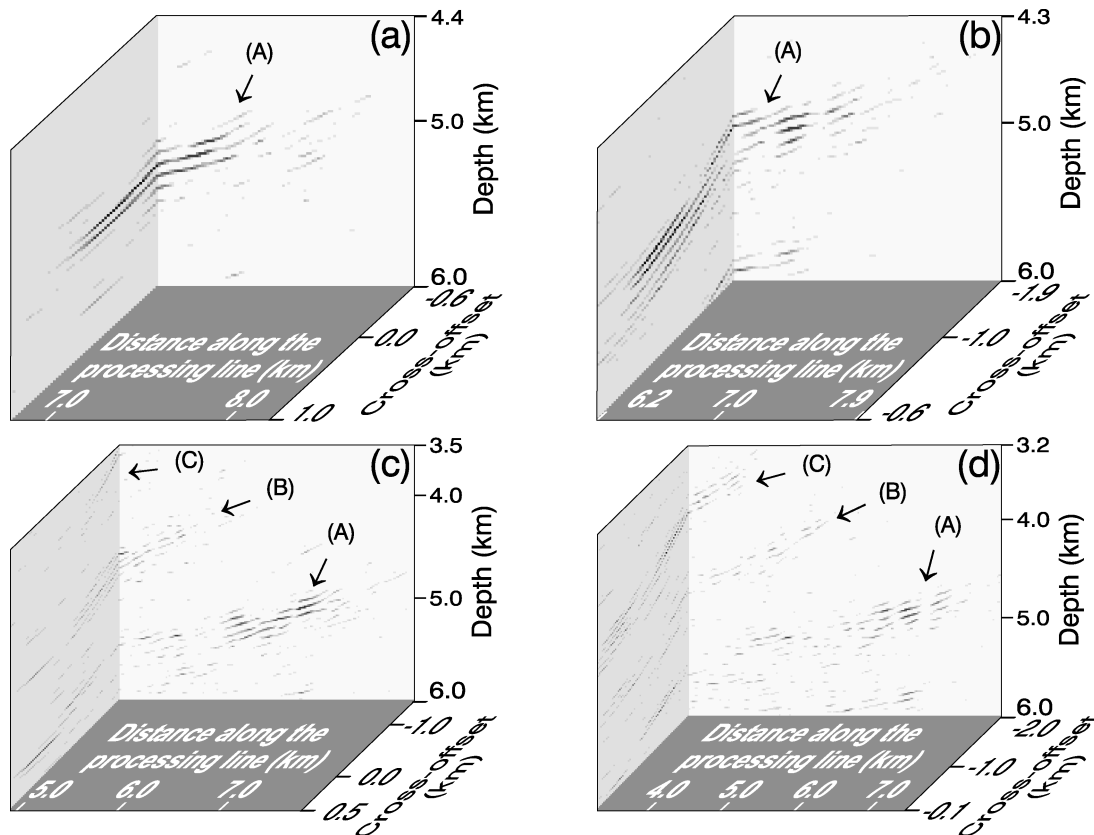

FIG. 10. Close-ups of the main groups of events in the 3D prestack migrated volume of Sturgeon Lake line data. (a, b, c, d) Perspective views from the west of vertical variable density sections through event groups A, B, and C, parallel and perpendicular to the processing line. The labeled reflectors clearly exhibit both in-line and cross-line dip. Views (a) and (b) are magnified more than views (c) and (d).

were shown in the optimum cross-dip stack example of Part I (Figure 8b). The results obtained by the two approaches agree with each other. Thus, the basic geologic interpretation given in Part I for the Sturgeon Lake line data and based on the optimum cross-dip stack is largely unchanged by the 3D result. Many details were better imaged by the 3D prestack migration, but their interpretation is beyond the scope of this paper.

To further emphasize the importance of extracting 3D structural information from 2D crooked-line survey data by using the methods presented here and in Part I, we compare various results obtained by migrating the Sturgeon Lake line data. Part of the migrated amplitude stack is shown in Figure 11b. The corresponding migrated standard stack is shown in Figure 11a. The migrated amplitude stack gives a better rendition of the relative strength of the reflectors and has better event continuity. The nominal resolution in the standard data is far superior, but most events have a multicyclic nature that makes any real structural resolution comparable to or worse than it is on the amplitude section. Although the migrated amplitude stack and migrated

standard stack are saturated with reflection events, both sections are misleading because most of the imaged events do not lie in the plane of the profile. This is confirmed by the 3D prestack migration result, which shows that most of the reflection events do not cross the plane of the processing line (see Figures 9 and 10) and much of what is imaged in this section is migration noise (Figure 11c). Similar results are obtained by 3D poststack migration of the optimum cross-dip stack. In view of the above, the main goal when processing swath 3D data is to extract the true reflector positions via the optimum cross-dip stack and/or 3D prestack migration. The conventional and amplitude stacks and their migrated counterparts should be used only when extracting 3D structural information fails.

SUMMARY AND CONCLUSIONS

In Part I, we explored methods for dealing with cross-dip problems in 2D processing of crooked-line data. Here we have explored the ability of 3D Kirchhoff prestack migration to solve the problem of correctly positioning all of the observed reflectors in 3D space. Our experiments on synthetic and field data indicate that, despite the limited cross-profile aperture of a typical crooked-line survey and the irregular distribution of midpoints in space, the method works quite well. Its principal disadvantage is the very large computational cost relative to any kind of 2D processing.

We also compared 3D migration of the full prestack data set with a simpler 3D poststack migration of the 2D locally optimum cross-dip stack of the data. Tests on synthetic data showed a high correlation between results from the two methods, both delineating the 3D geometry of the test reflectors quite well. But dropouts arise when the reflection responses from variously oriented reflectors overlap on the optimum cross-dip stack. Thus, one can expect to obtain better images by using the full prestack migration, but at much higher CPU cost.

Furthermore, we have shown that 2D amplitude sections are imaged by using standard 2D migration techniques. Amplitude stacking and migration seem to be more tolerant of time errors in the data than the usual methods. However, we only suggest amplitude processing of 2D crooked-line data as a last resort when extraction of 3D information by other techniques has failed.

Finally, there is no doubt that additional source points located off the acquisition line on any available side roads could improve the 3D imaging. Since adding a few source points is fairly inexpensive, such a strategy should be considered by future surveyors.
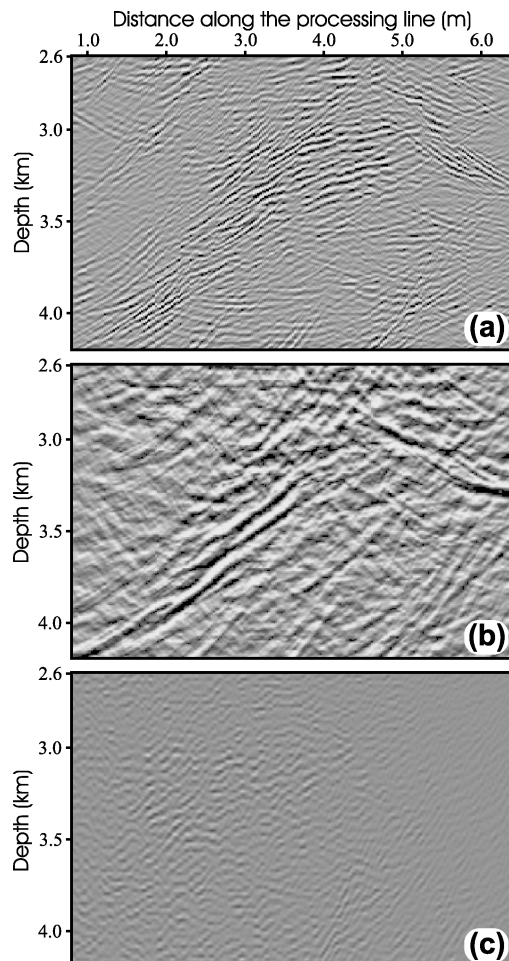

Fig. 11. Comparison of various migration results obtained from Sturgeon Lake line data. (a) Standard stacking and migration. (b) Amplitude stacking and migration. (c) The corresponding part of the slice across the processing line extracted from the 3D prestack migrated data volume.

ACKNOWLEDGMENTS

REFERENCES

Bancroft, J. C., Geiger, H. D., and Margrave, G. F., 1998, The equivalent offset method of prestack time migration: Geophysics, **63**, 2042–2053.

Geiger, H. D., Bancroft, J. C., and Foltinek, D., 1995, Prestack migra-

tion of crustal data using common scatterpoint (CSP) migration technique: Nat. Conv., Can. Soc. Expl. Geophys., Expanded Abstracts, 49–50.

Nedimovic, M. R., and West, G. F., 2003, Crooked-line 2D seismic reflection imaging in crystalline terrains: Part 1, data processing: Geophysics, **68**, 274–285, this issue.